phys. stat. sol. (b) **199**, 33 (1997)

Subject classification: 61.72.Cc; 68.55.Ln; S5.11; S5.12; S7.11; S7.12

Modeling of Threading Dislocation Density Reduction in Heteroepitaxial Layers

II. Effective Dislocation Kinetics¹)

A. E. ROMANOV²) (a), W. POMPE (a), G. BELTZ (b), and J. S. SPECK (c)

- (a) Arbeitsgruppe Mechanik Heterogener Festkörper, Max Planck Gesellschaft, Hallwachsstr. 3, D-01069 Dresden, Germany
- (b) Mechanical Engineering Department and
- (c) Materials Department, University of California, Santa Barbara, CA 93106, USA

(Received July 15, 1996)

The "effective kinetics" of threading dislocations (TDs) in growing epitaxial films is developed on the basis of the crystallographic and geometrical considerations from Part I of the paper. A system of coupled first-order nonlinear differential equations for twenty-four families of TDs is derived and solved for several initial conditions for TD densities. Numerical solutions demonstrated two general types of asymptotic behavior with increasing film thickness: linear decrease or saturation of total TD density. This behavior agrees with experimental data on TD reduction in mismatched homogeneous buffer layers.

1. Introduction

In Part I of this paper [1] a simple geometrical approach was developed to explain the experimentally observed 1/h scaling behavior for the threading dislocation (TD) density with the film thickness h for mismatched epitaxial buffer layers [2 to 4]. The approach was based on the idea of effective motion of inclined TDs along the film surface as a result of film growth and subsequent reactions between TDs. These reactions are annihilation, fusion, or scattering of TDs and are associated with a characteristic distance for initiating a reaction: r_A , r_F , and r_S , respectively. Additionally, in Part I, the crystal geometry of TDs and the possible reactions between them was developed for (001) epitaxial growth of (001) semiconductor films. It was argued that for this geometry twenty-four unique Burgers vector/slip plane combinations exist (which are included in Table I.1³)).

In this part of the paper, we treat the derivation and numerical solutions of the systems of coupled differential equations for "kinetics" of twenty-four TD families that is appropriate for the (001) growth of f.c.c. semiconductor films. It will be demonstrated that there exist two fundamental types of solutions for the coupled series of equations. The first type corresponds to the 1/h scaling dependence and describes balanced TD

¹) Part I see phys. stat. sol. (b) **198**, 599 (1996).

²⁾ Permanent address: A. F. Ioffe Physico-Technical Institute, Russian Academy of Sciences, 194 021 St. Petersburg, Russia.

³) We will use the Roman numeral "I" to denote tables, figures, and equations from Part I of this paper. Furthermore, the often referenced table in Part II will be designated as "Table II.1" so as to distinguish it from Table I.1.

distributions, that is, when the net Burgers vector content of all TDs is zero. The second type of solutions is applicable to non-balanced TD populations and predicts saturation behavior for TD densities at large film thicknesses. The saturation behavior corresponds to the experimental data presented in Part I.

2. Derivation of the Governing Equations for TD Reduction

In the development of equations for TD kinetics, we consider the example of TDs belonging to the family designated "1" in Table I.1 with density ϱ_1 , that is, for dislocations with Burgers vector $\mathbf{b}_1 = a/2[101]$ and line direction \mathbf{l}_1 approximately parallel to $[2\bar{1}3]$. First, we write the terms responsible for diminishing dislocation density. In the general case, all reactions of the type 1-j for $j=1 \rightarrow 24$ (see (I.22)) can contribute to the process of ϱ_1 decreasing,

$$\frac{\mathrm{d}\varrho_1}{\mathrm{d}h} = -\sum_{j=1}^{24} K_{1j}\varrho_1\varrho_j,\tag{1}$$

where ϱ_j is the density of TDs in the *j*-th family. K_{ij} are the "kinetic" coefficients that describe the "rate" of reactions between dislocations from families *i* and *j*. These coefficients are uniquely determined by the geometry of mutual motion of interacting dislocations and by characteristic distances, the interaction radii $r_{\rm I}$. The general expression for K_{ij} was found in Part I (see (I.24)).

The possible reactions between TDs are annihilation, fusion, and scattering. Here we will take into account only the first two reactions, with characteristic radii $r_{\rm A}$ and $r_{\rm F}$, respectively. Details of the formalism associated with scattering reactions are presented in Appendix A. As derived in Part I and shown in Table I.1, TDs from family 1 can only have annihilation reactions with TDs from family 4. TDs from family 1 can have fusion reactions with TDs from families 11, 12, 15, 16, 19, 20, 23, and 24. Therefore, only reactions with these families will contribute to the process of diminishing the density of TDs from family 1, i.e.,

$$\frac{\mathrm{d}\varrho_{1}}{\mathrm{d}h} = -K_{1,4}\varrho_{1}\varrho_{4} - K_{1,11}\varrho_{1}\varrho_{11} - K_{1,12}\varrho_{1}\varrho_{12} - K_{1,15}\varrho_{1}\varrho_{15} - K_{1,16}\varrho_{1}\varrho_{16}
- K_{1,19}\varrho_{1}\varrho_{19} - K_{1,20}\varrho_{1}\varrho_{20} - K_{1,23}\varrho_{1}\varrho_{23} - K_{1,24}\varrho_{1}\varrho_{24}.$$
(2)

It follows from the analysis of Table I.1 that TDs from family "1" may be generated only as the product of fusion reactions between TDs from the following pairs of families: 13–17, 13–18, 14–17, 14–18. Therefore, for *production* of TDs from family 1 as a result of fusion, one can write

$$\frac{\mathrm{d}\varrho_1}{\mathrm{d}h} = K_{13,17}\varrho_{13}\varrho_{17} + K_{13,18}\varrho_{13}\varrho_{18} + K_{14,17}\varrho_{14}\varrho_{17} + K_{14,18}\varrho_{14}\varrho_{18} \,. \tag{3}$$

Combining the generation of TDs as a result of fusion (3) with TD reduction as a result of annihilation and fusion (2) we arrive at the governing differential equation for the density of TD family 1, ϱ_1 , in the absence of scattering reactions

$$\frac{\mathrm{d}\varrho_{1}}{\mathrm{d}h} = -K_{1,4}\varrho_{1}\varrho_{4}
-\varrho_{1}(K_{1,11}\varrho_{11} + K_{1,12}\varrho_{12} + K_{1,15}\varrho_{15} + K_{1,16}\varrho_{16} + K_{1,19}\varrho_{19} + K_{1,20}\varrho_{20} + K_{1,23}\varrho_{23}
+ K_{1,24}\varrho_{24}) + K_{13,17}\varrho_{13}\varrho_{17} + K_{13,18}\varrho_{13}\varrho_{18} + K_{14,17}\varrho_{14}\varrho_{17} + K_{14,18}\varrho_{14}\varrho_{18}.$$
(4)

Similar equations can be readily derived for all twenty-four dislocation families. These twenty-four equations will include in the most general case 252 coefficients K_{ij} . These coefficients can be directly calculated from (I.24), however, some physical arguments and assumptions permit us to restrict the number of independent coefficients by taking into account the symmetry of the problem. First of all, by definition, $K_{ij} = K_{ji}$. Other relations between K_{ij} follow from Fig. I.4b where the crystallography of TDs for the case of (001) epitaxy is presented. For example, we conclude that

$$K_{2,11} = K_{6,15} = K_{4,9} = K_{5,12} = \dots,$$

 $K_{1,4} = K_{2,3} = K_{9,12} = K_{10,11} = \dots,$
 $K_{21,24} = K_{22,23} \dots,$ (5)

and so on. For the sake of simplicity, we assume an identical value for the coefficients $K_{ij} = D$ for all fusion reactions and that for the annihilation reaction $K_{14} = C$.

$$\frac{\mathrm{d}\varrho_{1}}{\mathrm{d}h} = -C\varrho_{1}\varrho_{4} - D\varrho_{1}(\varrho_{11} + \varrho_{12} + \varrho_{15} + \varrho_{16} + \varrho_{19} + \varrho_{20} + \varrho_{23} + \varrho_{24})
+ D(\varrho_{13}\varrho_{17} + \varrho_{13}\varrho_{18} + \varrho_{14}\varrho_{17} + \varrho_{14}\varrho_{18}).$$
(6)

We can rewrite (6) by including the coefficients $r_{\rm A}$ and $r_{\rm F}$,

$$\frac{\mathrm{d}\varrho_{1}}{\mathrm{d}h} = -r_{\mathrm{A}}c\varrho_{1}\varrho_{4} - r_{\mathrm{F}}d\varrho_{1}(\varrho_{11} + \varrho_{12} + \varrho_{15} + \varrho_{16} + \varrho_{19} + \varrho_{20} + \varrho_{23} + \varrho_{24})
+ r_{\mathrm{F}}d(\varrho_{13}\varrho_{17} + \varrho_{13}\varrho_{18} + \varrho_{14}\varrho_{17} + \varrho_{14}\varrho_{18}),$$
(7)

where c and d are dimensionless parameters that depend on the relative dislocation motion with changing film thickness. For example, it follows from (I.24) that for annihilation reactions (in the approximation that dislocations have $\sim \langle 112 \rangle$ line directions) $c = 2\sqrt{2}$ (for more realistic line directions, such as $\sim \langle 123 \rangle$, c will have a smaller value). For fusion reactions, we may also consider situations in which $c \approx d$. Finally, we can represent (7) in dimensionless form,

$$\frac{\mathrm{d}\tilde{\varrho}_{1}}{\mathrm{d}\tilde{h}} = -c\tilde{\varrho}_{1}\tilde{\varrho}_{4} - c\varkappa\tilde{\varrho}_{1}(\tilde{\varrho}_{11} + \tilde{\varrho}_{12} + \tilde{\varrho}_{15} + \tilde{\varrho}_{16} + \tilde{\varrho}_{19} + \tilde{\varrho}_{20} + \tilde{\varrho}_{23} + \tilde{\varrho}_{24})
+ c\varkappa(\tilde{\varrho}_{13}\tilde{\varrho}_{17} + \tilde{\varrho}_{13}\tilde{\varrho}_{18} + \tilde{\varrho}_{14}\tilde{\varrho}_{17} + \tilde{\varrho}_{14}\tilde{\varrho}_{18}),$$
(8)

where $\tilde{h} = h/r_A$, $\tilde{\varrho}_i = \varrho_i r_A^2$, and $\varkappa = r_F/r_A$ and now d = c. Using the same approximations and designations, we can write the equations for the rest of the TD densities (see Appendix B). The derived system of coupled ordinary nonlinear differential equations will serve as the basis for the analysis of TD kinetics in growing films under different initial conditions.

3. Numerical Solutions and Interpretation

The numerical solutions of the system of coupled differential equations for TD densities, (B1) to (B24), can be obtained using standard mathematical software. We will illustrate the possible behavior of TD densities by several examples of solutions for different initial conditions which are listed in Table II.1. Two groups of possible initial conditions should be treated separately. The parameter responsible for this subdivision is the net Burgers

		Table 1	e I																					
		Initial Burge	Initial TD densities Burgers vector cont	densit tor co	ies foi ntent	$(\mathbf{B} =$	nerica 0). T	l solui he un	ions balan	to cor ced ca	upled ses (N	differe	ntial . V8) co	equati rrespo	ions.	Initial TD densities for numerical solutions to coupled differential equations. The first eight cases (B1 to B8) correspond to zero net Burgers vector content ($\mathbf{B} = 0$). The unbalanced cases (N1 to N8) correspond to a net Burgers vector content ($\mathbf{B} \neq 0$)	eight ırgers	cases	(B1 ta conter	o B8)	corres $\neq 0$)	puods	to zei	o net
	$\tilde{\varrho}_1^0$	$\tilde{\mathfrak{Q}}_2^0$	$\tilde{\varrho}_3^0$	$\tilde{\varrho}_4^0$	$\tilde{\varrho}_5^0$	$\tilde{\mathfrak{Q}}_6^0$	$\tilde{\mathbb{Q}}_{7}^{0}$	$\tilde{\mathfrak{Q}}_8^0$	\tilde{Q}_9^0	$\tilde{\varrho}_{10}^0$	$\tilde{\varrho}_{11}^0$	$\tilde{\varrho}_{12}^0$	$\tilde{\varrho}_{13}^0$	$\tilde{\varrho}_{14}^0$	$\tilde{\varrho}_{15}^0$	$\tilde{\varrho}_{16}^0$	$\tilde{\varrho}_{17}^0$	$\tilde{\varrho}_{18}^0$	$\tilde{\varrho}_{19}^0$	$\tilde{\mathfrak{Q}}_{20}^0$	$\tilde{\varrho}_{21}^0$	$\tilde{\varrho}_{22}^0$	$\tilde{\mathfrak{Q}}_{23}^0$	$\tilde{\varrho}_{24}^0$
_	0.025	0.025	0.025 0.025 0.025 0.025	0.025		0.025 0.025 0.025	0.025	0.025	0.02	0.025	0.025 0.025 0.025 0.025	0.025	0.025	0.025 0.025 0.025 0.025	0.025	0.025	0	0	0	0	0	0	0	0
B2	0.025	0.025	0.025	0.025		0.030	0.030	0.030	0.02	0.02	0.025	$0.030 \ 0.030 \ 0.030 \ 0.030 \ 0.025 \ 0.025 \ 0.025 \ 0.025 \ 0.025 \ 0.025 \ 0.025$	0.025	0.025	0.025	0.025	0	0	0	0	0	0	0	0
B3	0	0	0 0 0 0	0	0	0	0	0	0	0	0	0	0	0	0	0	0.025	5 0.025	0.025	0.025	0.025	$0.025 \ 0.025$	0.025	0.025
B4	0	0	0	0	0	0			0		0			0	0	0	0.05	$0.025 \ 0.025$	0.025	0.025	0.030	0.030 0.030	0.030	0.030
B5	0.025	0.025	0.025	0.025		$0.025\ 0.025\ 0.025$	0.025		$0.025 \ 0.025$	0.025	0.025	0.025	0.025	0.025	0.025	0.025 0.025	0.025	5 0.025	0.025	0.025	0.025	$0.025\ 0.025\ 0.025$		0.025
B6	0.025	0.025	0.025 0.025 0.025 0	0.025		$0.030 \ 0.030 \ 0.030$	0.030	0.030	0.025	0.02	0.025	$0.025\ 0.025\ 0.025$	0.025	0.025		$0.025 \ 0.025$	0.028	$0.025 \ 0.025$	0.025	0.025	0.035	$0.035\ 0.035\ 0.035$		0.035
B7	0.025	0	0.025	0	0.025	0.025 0	0.025	0 9	0.025	0	0.025	0	0.025	0	0.025	0	0	0	0	0	0	0	0	0
B8	0.025	0.025	$0.025 \ 0.025 \ 0.035$	0.035		0.025	0.025	$0.025 \ 0.025 \ 0.025 \ 0.025 \ 0.025$	0.02	0.02	0.025	$0.025\ 0.025\ 0.025$		$0.035 \ 0.035$		$0.025 \ 0.025$	0	0.020	0	0	0		0	0
N_1	0.030	0.030	0.025	0.025		0.025 0.025 0.025	0.025	0.025	0.02	0.02	0.025 0.025 0.025 0.025	0.025	0.025	0.025	0.025 0.025 0.025	0.025	0	0	0	0	0	0	0	0
12	0.030	$0.030 \ 0.030$	0.025 (0.025		$0.020\ 0.020\ 0.025$	0.025	6.025	$0.025 \ 0.025$	0.02	0.025	$0.025\ 0.025\ 0.025$		$0.025 \ 0.025$	$0.025 \ 0.025$	0.025	0	0	0	0	0	0	0	0
N3	0	0	0	0	0	0	0	0	0	0	0	0	0	0	0	0	0.030	0.030	0.025	0.025	0.025	$0.025\ 0.025\ 0.025$		0.025
74	0	0	0	0	0	0			0	0	0	0	0	0	0	0	0.030	0.030	0.025	0.025	0.020	0.020	0.025	0.025
N_5	0.030	0.030	0.025	0.025	0.020	$0.020\ 0.020\ 0.025$	0.025	6.025	0.02	0.02	0.025	$0.025\ 0.025\ 0.025\ 0.025\ 0.025$	0.025	$0.025\ 0.025\ 0.025\ 0.025$	0.025	0.025	0.030	0.030	0.025	$0.025 \ 0.025$	0.020	$0.020\ 0.020\ 0.025$	0.025	0.025
91	0.010	0.010	0.010 0.010 0 0	0	0	0	0	0	0	0	0	0	0	0	0	0	0.05($0.050 \ 0.050 \ 0.050 \ 0.050$	0.050	0.050	0		0	0
17	0.065	0.065	0.060	0.060	0.055	0.055	0.050	0.050	0.045	0.045	0.040	$0.055 \ 0.055 \ 0.050 \ 0.050 \ 0.045 \ 0.045 \ 0.040 \ 0.040 \ 0.035 \ 0.035 \ 0.030 \ 0.030$	0.035	0.035	0.030	0.030	0	0	0	0	0	0	0	0
8N	0.025 0	0	0.025	0.025	0.025	$0.025 \ 0.025 \ 0.025$	0.025	0.025	0.025	0.025	0.025	$0.025 \ 0.025 \ 0.025 \ 0.025 \ 0.025$	0.025	$0.025 \ 0.025$		0.025 0.025	0	0	0	0	0		0	0

vector content **B** of the TDs in the film, defined as

$$\mathbf{B} = \sum_{i=1}^{24} \tilde{\varrho}_i^0 \mathbf{b}_i \,, \tag{9}$$

where $\tilde{\varrho}_i^0$ are the normalized TD densities for the initial thickness h_0 , and \mathbf{b}_i is the Burgers vector of a TD from the *i*-th family. We note that the net Burgers vector content \mathbf{B} of the TDs is a conserved vector that can be distributed amongst several specific TD families.

3.1 Balanced TD densities (B = 0)

3.1.1 Relation between growth structure and initial conditions

The first group of initial conditions (cases B1 through B8 in Table II.1) correspond to "balanced" cases; i.e., the TDs in the film have no net Burgers vector content ($\mathbf{B}=0$). This can happen when the families with opposite Burgers vectors $+\mathbf{b}$ and $-\mathbf{b}$ have equal initial densities (cases B1 through B7). Special attention has to be given to case B7 for which TDs with the same Burgers vector, but from different slip systems, have equal initial densities. The other special example is presented for case B8 where there is no equilibrium between some $+\mathbf{b}$ and $-\mathbf{b}$ pairs ($\tilde{\varrho}_1^0 = \tilde{\varrho}_2^0 \neq \tilde{\varrho}_3^0 = \tilde{\varrho}_4^0$, $\tilde{\varrho}_{13}^0 = \tilde{\varrho}_{14}^0 \neq \tilde{\varrho}_{15}^0 = \tilde{\varrho}_{16}^0$, and $\tilde{\varrho}_{18}^0 \neq \tilde{\varrho}_{19}^0$) but the global condition $\mathbf{B}=0$ is maintained.

Cases B1 and B2 in Table II.1 correspond to the presence of populations of TDs with inclined Burgers vectors with respect to the film/substrate interface and zero populations of TDs with Burgers vectors parallel to the film/substrate interface. Such a situation can result from surface nucleated TDs during layer-by-layer film growth. In case B1, all TD populations have the same initial densities that correspond to a uniform generation of dislocations by surface sources. In case B2, populations $5 \rightarrow 8$ have higher densities than other TDs. This may happen, for example, as a result of heterogeneous stresses, or an imperfect biaxial stress state. For cases B3 and B4, initially TDs with their Burgers vector parallel to the film/substrate interface are present. This dislocation configuration may be a consequence of coalescence of impinging islands. Case B5 is a combination of cases B1 and B3; similarly, case B6 is a combination of cases B2 and B4. Regarding case B7, we propose that this initial TD configuration may be formed due to an artifically-induced imbalance between slip systems. Finally, case B8 represents a situation that does not correspond to any particular TD formation mechanism, but may be of interest from an academic point of view.

3.1.2 Numerical solutions

Examples of numerical solutions of the equations for TD kinetics in growing films for the balanced cases are presented in Fig. 1 and 2 (for these figures, the values of the parameters c=2 and $\varkappa=1$ were used for the numerical solution of the system of equations (B1) to (B24)). All families follow a 1/h dependence for large film thicknesses h and converge to a single curve. However, at the initial stage of film growth the behavior of specific TD densities may be different. For example, case B1 (see Fig. 1, upper panel) corresponds to an idealized situation where all TDs are generated by surface nucleation of half-loops. For these initial conditions, the TD densities ϱ_1 through ϱ_{16} decrease monotonically with increasing film thickness. In contrast, TD densities ϱ_{17} through ϱ_{24}

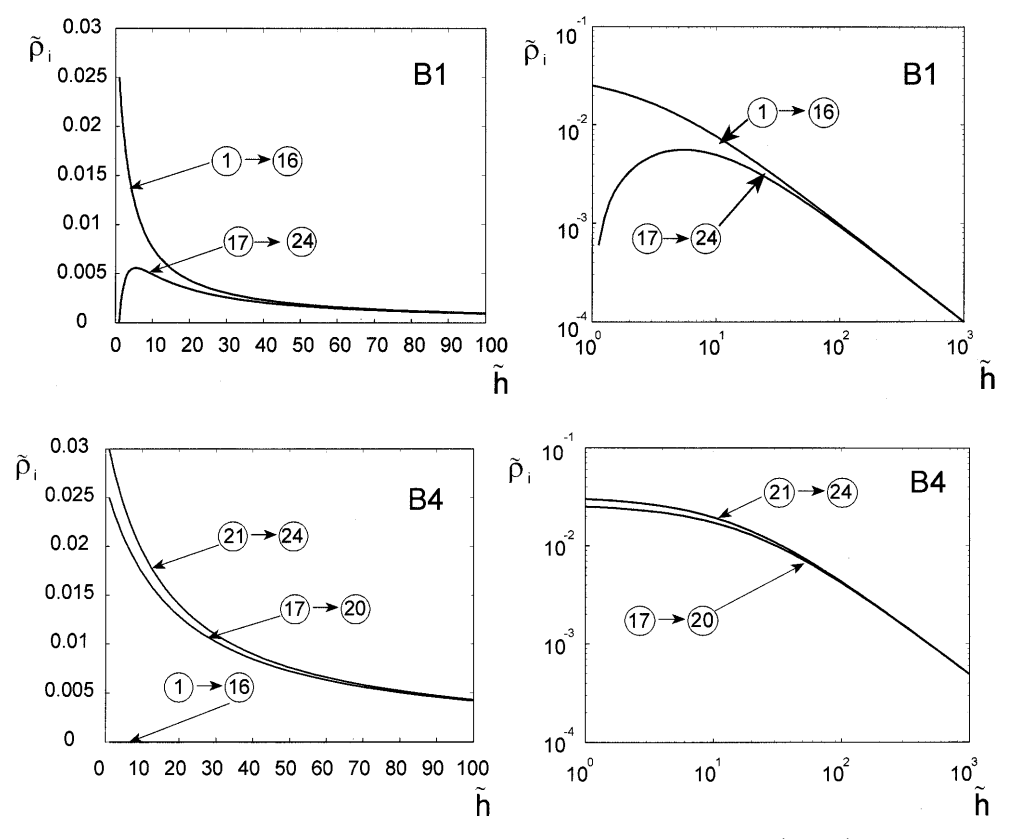


Fig. 1. Threading dislocation densities for balanced Burgers vector content ($\mathbf{B}=0$) corresponding to surface nucleated TDs (case B1 from Table II.1) (upper panel) and to TDs generated during island coalescence (case B4 from Table II.1) (lower panel). Left column: linear–linear scale; right column: log–log scale. The specific TD designation is indicated in the figure and in Table I.1; c=2 and $\varkappa=1$

show a rapid initial increase and then also begin to decrease with increasing film thickness. The initial increase in TD densities ϱ_{17} through ϱ_{24} is due to fusion reactions between primary TDs (surface nucleated TDs). With increasing thickness, the densities ϱ_{17} through ϱ_{24} reach a maximum value at $\tilde{h}\approx 5$, and at a thickness of $\tilde{h}\approx 100$, the TD densities converge for all families.

An idealized case of island growth, where the TDs are generated as a result of island coalescence, is shown in Fig. 1, lower panel. In this balanced case ($\mathbf{B} = 0$), families 17 through 20 have a smaller initial density than families 21 through 24. The difference in densities diminishes with increasing thickness as a result of higher initial concentration of TDs in families 21 through 24 and thus a higher initial rate of annihilation.

The mixed case, in which all types of TDs are initially present in equal densities (for example case B5 shown in Fig. 2, upper panel), demonstrates the identical monotonic decrease in density for all families. Families 1 through 24 have been treated equivalently in (B1) to (B24), and thus with equal initial conditions, the system maintains this equivalence in TD densities. However, if the symmetry of the initial conditions is bro-

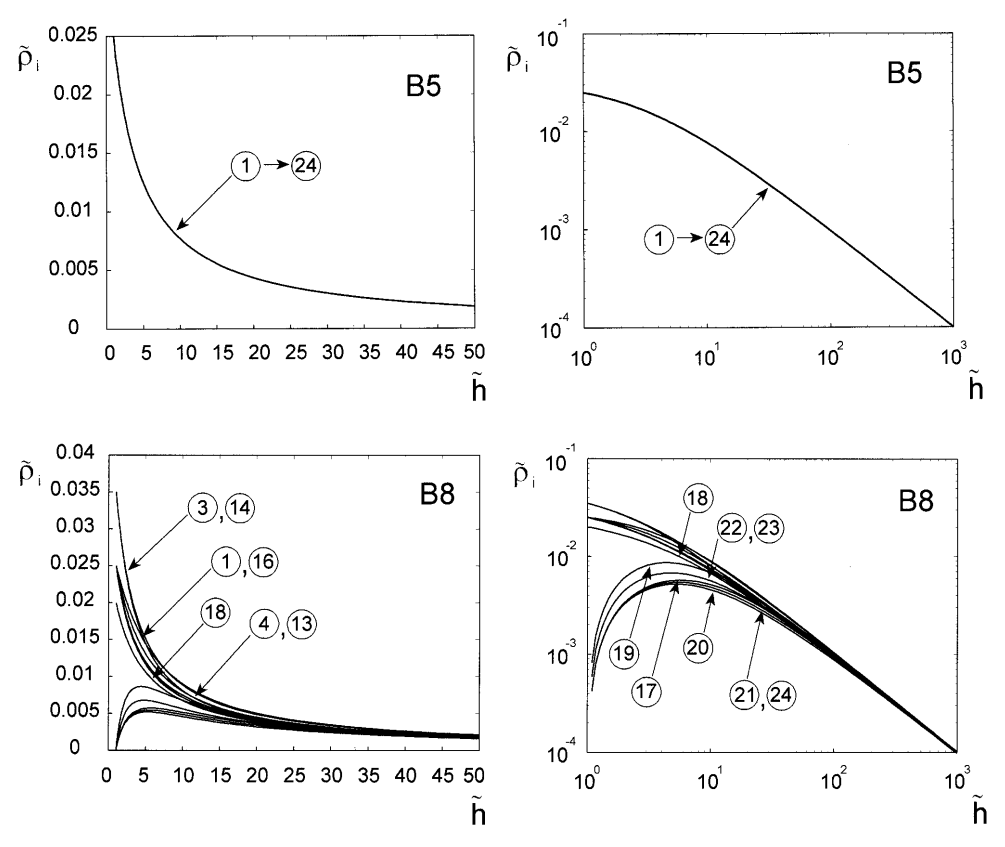


Fig. 2. Threading dislocation densities for balanced Burgers vector content ($\mathbf{B}=0$) corresponding to TDs for cases B5 (upper panel) and B8 (lower panel) from Table II.1. These TDs correspond to those for a mixed growth mode. Left column: linear–linear scale; right column: log–log scale. The specific TD designation is indicated in the figure and in Table I.1; c=2 and $\varkappa=1$

ken, as in case B8 (Fig. 2, lower panel), then there is a "transition thickness" necessary for all of the families to converge to the same value for increasing h. Similar to case B1, some families show an increasing initial TD density as a result of fusion reactions.

3.1.3 Thickness dependence of total TD density

For the balanced cases, the total TD density $\tilde{\varrho}_{\rm T} = \sum_{i=1}^{24} \tilde{\varrho}_i$ always obeys the 1/h dependence at large film thicknesses. This can be easily seen from the log-log plot in Fig. 3a. Note that in this plot, the ordinate is the logarithm of the relative TD density, i.e., $\tilde{\varrho}_{\rm T}/\tilde{\varrho}_{\rm T}^0$, where $\tilde{\varrho}_{\rm T}^0 = \varrho_{\rm T}^0 r_{\rm A}^2$ and $\varrho_{\rm T}^0$ is the initial total TD density, and thus the offset of the curves at large h is simply log $(\tilde{\varrho}_{\rm T}^0)$, which will be discussed shortly. From the analysis of Fig. 3a, and in close analogy with (I.10), we propose that the behavior of the total TD density $\varrho_{\rm T}$ in balanced cases may have the following dependence:

$$\varrho_{\mathrm{T}} = \frac{\tilde{\varrho}_{\mathrm{T}}}{r_{\mathrm{A}}^2} = \frac{1}{K_{\mathrm{T}}(h + \hat{h}_{\mathrm{T}})}$$

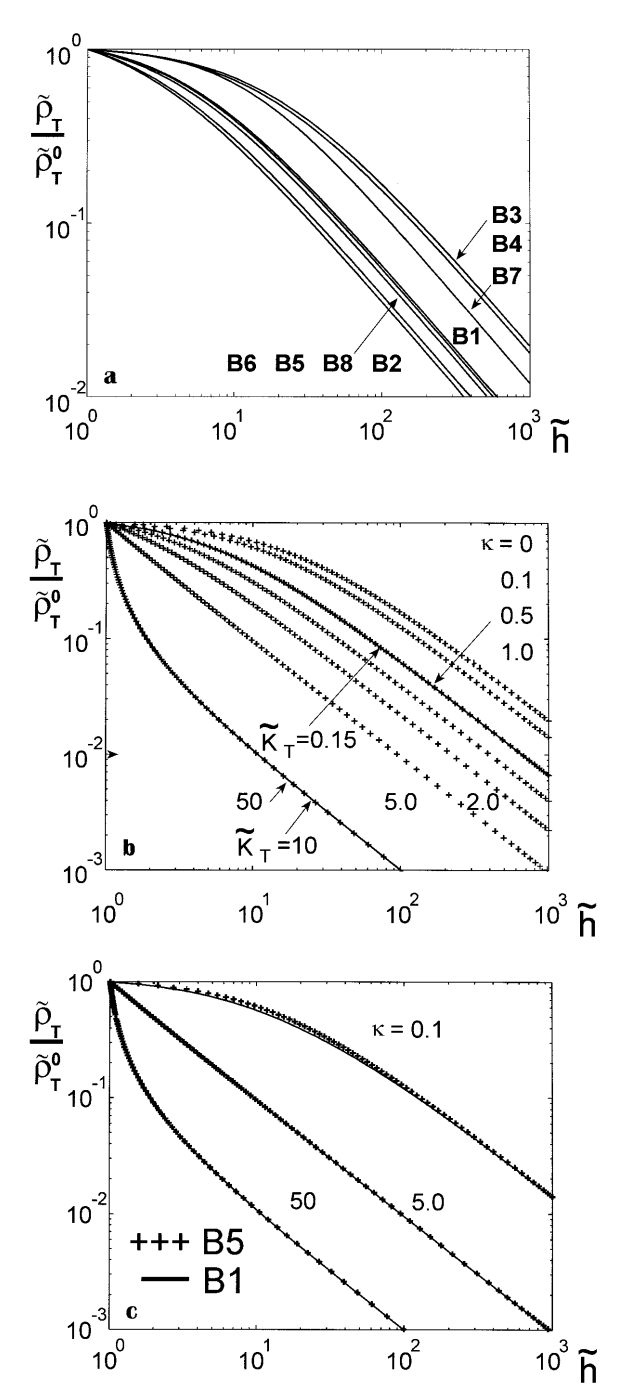


Fig. 3. Logarithmic plots of the total relative threading dislocation densities as a function of normalized film thickness for balanced cases ($\mathbf{B} = 0$). a) Dependencies for different initial conditions given in Table II.1; c=2 and $\varkappa = 1$. b) Dependencies for different values of the relative radius for fusion \varkappa , c=2 (case B1 from Table II.1). The \varkappa values are indicated in the figure. Solid lines represent solutions obtained with the help of (10). $\tilde{K}_{\rm T}$ values are indicated in the figure. c) Dependencies for different values of \varkappa for case B5 (+) and normalized case B1 (solid lines) such that the total initial TD density $\tilde{\varrho}_{\mathrm{T}}^{0}=0.6$ for both cases. The geometric parameter c=2was used for these solutions

$$\log \frac{\tilde{\varrho}_{\mathrm{T}}}{\tilde{\varrho}_{\mathrm{T}}^{0}} = -\log \left[\tilde{K}_{\mathrm{T}} (\tilde{h} - \tilde{h}_{0}) + 1 \right], \tag{10}$$

where $K_{\rm T}$ is the global TD "kinetic reaction" coefficient (and $\tilde{K}_{\rm T} = K_{\rm T} \varrho_{\rm T}^0 r_{\rm A}$ is its normalized value), $\hat{h}_{\rm T} = 1/(K_{\rm T} \varrho_{\rm T}^0) - h_0$, and $\tilde{h}_0 = h_0/r_{\rm A}$. Clearly, (10) correctly predicts the behavior of the total TD density for $h \gg \hat{h}$; the value of the coefficient $\tilde{K}_{\rm T}$ can be found from the extrapolation of the linear parts of the curves in Fig. 3a to the value at $\log \tilde{h} = 0$. To confirm

the general dependence of (10) for any film thickness, we first need to examine other features of the solution of the general system of differential equations.

3.1.4 Competition between annihilation and fusion reactions

We reiterate that the results presented in Fig. 1 and 2, and correspondingly Fig. 3a, were obtained for c=2 and $\varkappa=1$ in (B1) to (B24). Recall here the results of Section 2 (also see Appendix B), where the parameter c was associated with the geometry of effective motion of TDs in growing films and \varkappa characterized the relative radius for fusion reactions with respect to the annihilation radius. From the structure of the system of equations (B1) to (B24), it is clear that a change of the parameter c will lead to a simple renormalization of the film thicknesses. That is, for larger c, the same values of $\tilde{\varrho}_i$ and $\tilde{\varrho}_T$ will be achieved for a smaller value of the film thickness b. This is because a larger value of c leads to larger dislocation motion for the prescribed change in film thickness.

The influence of the parameter \varkappa (the ratio of fusion radius to the annihilation radius) on the TD reduction is shown in Fig. 3b for initial TD densities given by case B5 in Table II.1. For larger \varkappa , the TD densities fall more rapidly, indicating that larger \varkappa corresponds to a larger global $\tilde{K}_{\rm T}$. This behavior can be understood in the framework of annihilation and fusion reactions. First, if we consider cases where the annihilation is the only possible reaction, $\varkappa=0$, then a TD from a specific family only has the possibility of reacting with TDs from one of the twenty-four families (Fig. 3b). However, in the case in which both fusion and annihilation are possible, then a TD from a specific family has the possibility of reacting with TDs from nine of the twenty-four families; one of these reactions will correspond to annihilation and eight to fusion. However, fusion between TDs from other families will lead to TD generation and for a specific family, there will exist four sets of generation reactions. For the case where fusion and annihilation have equal interaction radii, i.e., $\varkappa=1$, we expect the global $\tilde{K}_{\rm T}$ to be five times larger than for the case where $\varkappa=0$, as seen in Fig. 3b. Further, we note that the 1/h behavior can also be obtained when there is effectively only fusion, as seen in Fig. 3b for increasing values of \varkappa .

The validity of the general behavior (10) was checked for two very different values of \varkappa . For $\varkappa=0.5$ and 50 from the large thickness region (-1 slope in the log-log plots), $\tilde{K}_{\rm T}$ was found to be equal to 0.15 and 10, respectively. Since \tilde{h}_0 is defined by the initial conditions ($\tilde{h}_0=1$), the full predicted behavior for $\log \tilde{\varrho}_{\rm T}/\tilde{\varrho}_{\rm T}^0$ can be simply checked by plotting (10) for the values of $\tilde{K}_{\rm T}$ estimated above. The agreement for both \varkappa values is excellent, as shown in Fig. 3b.

The solutions in Fig. 3a correspond to unequal total initial densities $\tilde{\varrho}_{\rm T}^0$. To verify the offset of normalized TD density for a large normalized thickness in the plots of total TD density in Fig. 3a ("offset effect"), we have repeated the calculations for renormalized initial densities for case B1 in which the total density $\tilde{\varrho}_{\rm T}^0$ (= 0.6) for this modified case is equal to the total density for case B5. This normalization of total density leads to coincident curves for $\tilde{\varrho}_{\rm T}$ for cases B1 and B5 for several values of \varkappa , as shown in Fig. 3c. This result demonstrates both the offset effect is a consequence of total initial density and that the initial distribution of TDs over the families does not change the overall character of the solution.

3.2 Non-balanced TD densities $(B \neq 0)$

3.2.1 Basis for non-balanced TD densities

In the second group of initial conditions (cases N1 through N8 in Table II.1), the initial TD densities are not balanced such that the film has a net Burgers vector content ($\mathbf{B} \neq 0$). TD reactions happen locally, and in many cases on a local length scale, there

may be a local net Burgers vector content of TDs. However, globally, $\mathbf{B} = 0$ may or may not be achieved. The fluctuations in the net Burgers vector content thus become a very important topic for future investigations. Here, however, we treat the general case in which there is a net Burgers vector content and do not consider the origin of this behavior. Again, variations for the presence and absence of TDs with Burgers vectors parallel to the film/substrate interface are considered. The results show many similar features to the solutions for the balanced cases. However, since there is a net Burgers vector content, at least one, and often a set of families will show saturation behavior.

3.2.2 Numerical solutions

For the non-balanced situations, the initially prescribed net Burgers vector content is invariant with regard to film growth. An example of such behavior is given in Fig. 4, upper panel where $\varrho_1^0 = \varrho_2^0 > \varrho_i^0$ for i = 3 to 16 and TD families 17 through 24 (with Burgers vector parallel to the film/substrate interface) are initially absent. As in the bal-

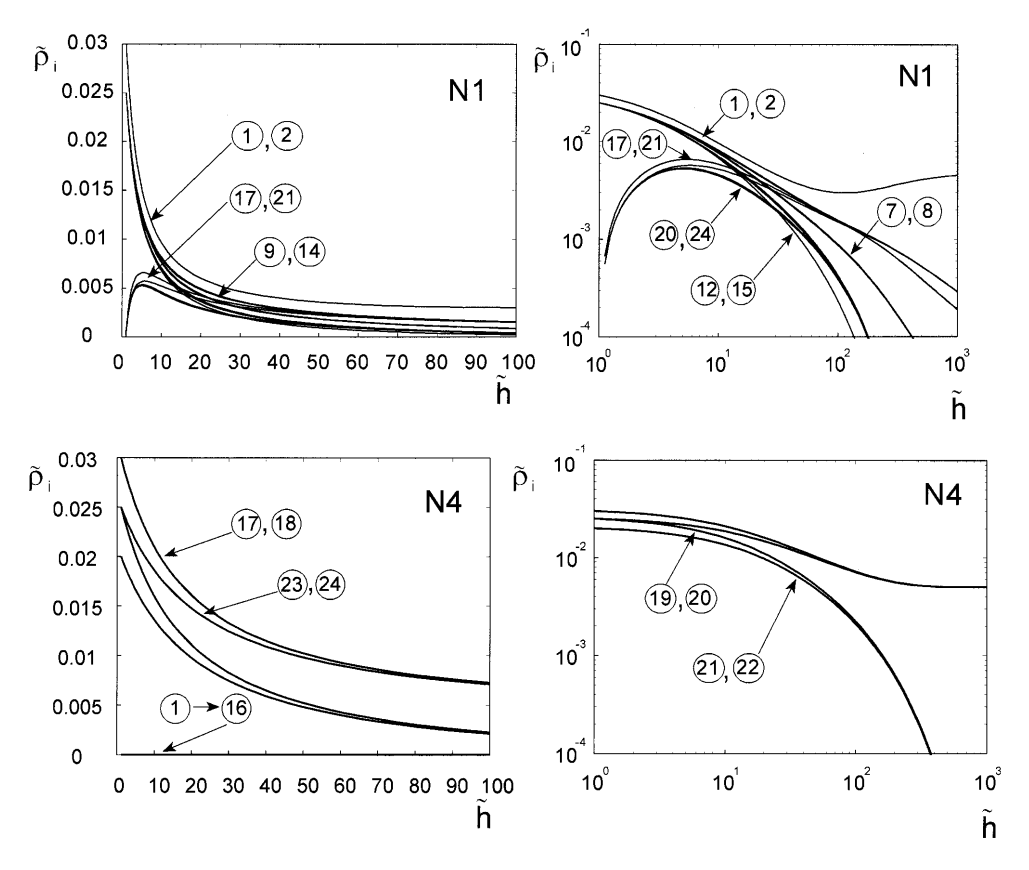


Fig. 4. Threading dislocation densities for non-balanced Burgers vector content ($\mathbf{B} \neq 0$) corresponding to surface nucleated TDs (case N1 from Table II.1) (upper panel) and to TDs generated during island coalescence (case N4 from Table II.1) (lower panel). Left column: linear–linear scale; right column: log–log scale. The specific TD designation is indicated in the figure and in Table I.1; c=2 and $\varkappa=1$

anced case, the densities of primary dislocations ϱ_1 through ϱ_{16} begin to decrease with increasing h due to both annihilation and fusion reactions. The densities of secondary dislocations ϱ_{17} through ϱ_{24} initially increase, but also fall with increasing film thickness. For larger values of \tilde{h} , ϱ_3 through ϱ_{16} asymptotically approach zero. However, ϱ_1 and ϱ_2 asymptotically approach saturation values $\Delta\varrho = \varrho_1 - \varrho_i$. The total density $\varrho_{\rm T}$ also saturates to a value $2\,\Delta\varrho$ because of the initial net Burgers vector content.

The other non-balanced cases (Fig. 4, lower panel and Fig. 5) present different situations where the saturation behavior manifests itself in the ensemble of TDs in growing films. For example, case N4 (Fig. 4, lower panel) corresponds to island growth, where only TDs with Burgers vectors parallel to the film/substrate interface exist and have an initial imbalance. In this case, the imbalance between pairs of TD families remains constant, i.e.,

$$(\varrho_{23} + \varrho_{24}) - (\varrho_{21} + \varrho_{22}) = (\varrho_{17} + \varrho_{18}) - (\varrho_{19} + \varrho_{20}) = 2 \Delta \varrho, \tag{11}$$

where $\Delta \varrho = \varrho_{23}^0 - \varrho_{22}^0 = \varrho_{17}^0 - \varrho_{21}^0$.

Fig. 5 corresponds to non-balanced cases in which there are TDs that may appear by both layer-by-layer and island growth. We note that for case N5 the TD behavior is similar

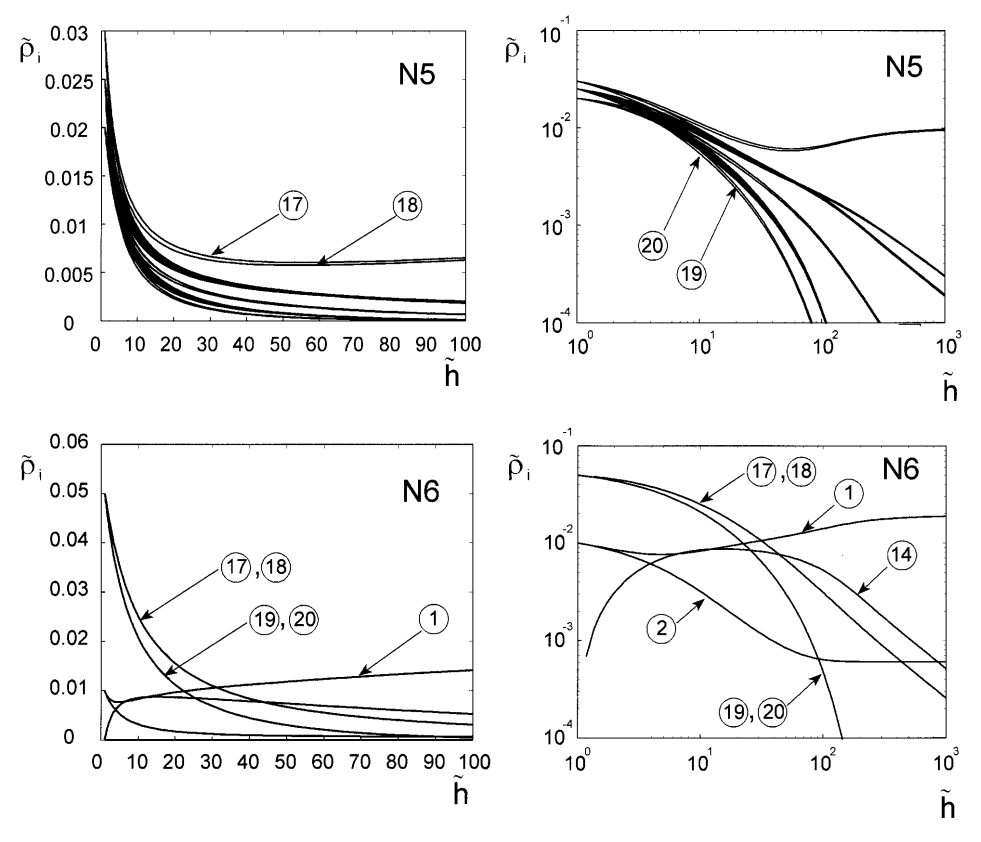
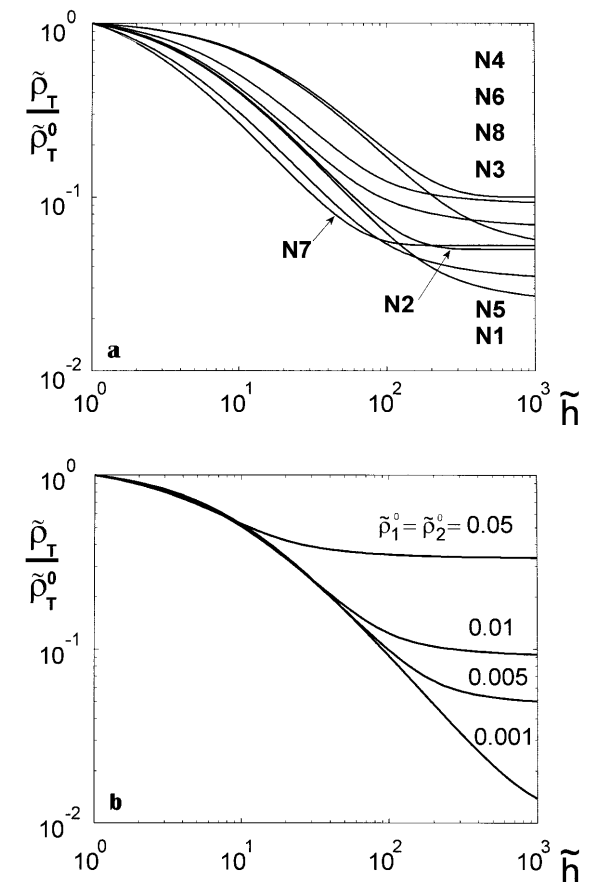


Fig. 5. Threading dislocation densities for non-balanced Burgers vector content ($\mathbf{B} \neq 0$) corresponding to TDs for case N5 (upper panel) and case N6 (lower panel) from Table II.1. These TDs correspond to those for a mixed growth mode. Left column: linear–linear scale; right column: log–log scale. The specific TD designation is indicated in the figure and in Table I.1; c=2 and $\varkappa=1$

to N1. Interestingly, the solutions for the initial conditions N5 correspond to twenty-four distinct values of the TD families (no pairing of families). For this case, $\mathbf{B} = 0.02 \, a/2[110]$ and for large h, the two families that saturate to a finite density are TD families 17 and 18, both with Burgers vector $\mathbf{b} = a/2[110]$ each with densities $\tilde{\varrho}_{17}^{\infty} = \tilde{\varrho}_{18}^{\infty} = 0.01$. The behavior of the solutions for case N6 (see Fig. 5, lower panel) demonstrates saturation in which a given excess of Burgers vectors is unequally distributed in the two families 1 and 2. This demonstrates that the net Burgers vector content is preserved yet redistributed into different families (line directions). This behavior can be understood in the framework of the fusion reactions between families with non-zero densities. We will use case N6 with different values of $\tilde{\varrho}_1^0 = \tilde{\varrho}_2^0$ to demonstrate some of the general features of saturation behavior.

3.2.3 Thickness dependence of the total TD density

The behavior of the total TD density for the non-balanced cases is shown in Fig. 6, where Fig. 6a summarizes all of the cases of initial conditions N1 through N8 and Fig. 6b demonstrates the saturation behavior for varying ratios $|\mathbf{B}|/\tilde{\varrho}_{\mathrm{T}}^{0}$. Notice in Fig. 6a that for a range of thicknesses, the TD density follows the 1/h scaling behavior and then saturates. The magnitude of the saturation value approximately scales as



 $|\mathbf{B}|/\tilde{\varrho}_{\mathrm{T}}^{0}$. Detailed considerations of the absolute magnitude of the saturation value $\tilde{\varrho}_{\mathrm{T}}^{\infty}$ depends on how \mathbf{B} is partitioned into individual components related to dislocation families. In Fig. 6b, we demonstrate this dependence of the change in saturation value with decreasing $|\mathbf{B}|/\tilde{\varrho}_{\mathrm{T}}^{0}$. Together with the decrease in saturation level, the 1/h region increases. Furthermore, the value of \tilde{K}_{T} is approximately independent of $|\mathbf{B}|/\tilde{\varrho}_{\mathrm{T}}^{0}$.

Fig. 6. Logarithmic plots of the total relative threading dislocation densities as a function of normalized film thickness for non-balanced cases ($\mathbf{B} \neq 0$). a) Dependencies for different initial conditions given in Table II.1, cases N1 through N8; c=2 and $\varkappa=1$. b) Dependencies for different magnitudes of the net Burgers vector content $|\mathbf{B}|$ (and correspondingly $\Delta\varrho$) for the case N6; $\varkappa=1,\ c=2$. The value of $\tilde{\varrho}_1^0=\tilde{\varrho}_2^0$ is indicated in the figure

4. Discussison and Conclusions

The results reported in this paper demonstrate that for initially balanced ($\mathbf{B}=0$) cases, the total TD density follows the global reduction law (10). The model presented in Part I treated only one type of TD density. It was shown here in Part II that the total reduction is described by the coefficient $\tilde{K}_{\rm T}$. This result appears to be valid at least for situations when the series of differential equations includes only a single parameter for the geometry of TD motion (parameter c) and two parameters for TD reactions: the annihilation radius $r_{\rm A}$ and the fusion radius $r_{\rm F}$.

We have also demonstrated that for balanced cases the total TD density $\varrho_{\rm T}(h)$ appears to be independent of the initial distribution of TDs between different subfamilies. We conclude that $\tilde{K}_{\rm T}$ in (10) depends on the value of \varkappa and thus on the possibility of fusion reactions within an ensemble of TDs. When fusion is not possible due to initial conditions, for example if only the TDs of the initially present families have Burgers vectors that lie in the plane of the film/substrate interface (e.g., see case B4), then the value of $\tilde{K}_{\rm T}$ corresponds to that of $\varkappa = 0$. In the general case, however, varying the ratio of $r_{\rm F}$ to $r_{\rm A}$ (parameter \varkappa) does not change the global behavior for the balanced cases; rather, increasing \varkappa only increases the overall rate of reduction by increasing the value of $\tilde{K}_{\rm T}$.

For non-balanced TD distributions ($\mathbf{B} \neq 0$), the total TD density shows the same initial behavior as the balanced cases. However, at large film thickness, $\tilde{\varrho}_{\mathrm{T}}$ saturates to a constant value. The saturation behavior is due to the net Burgers vector content \mathbf{B} which is defined by (9). The main characteristic of \mathbf{B} is that it remains constant during reactions in a TD ensemble, however, it can be redistributed amongst several TD families. We believe that saturation in real experiments [5] is a consequence of lateral fluctuations in the density of different TD families and thus fluctuations in \mathbf{B} .

The treatment presented in Part II provides new insight into the details of TD reduction. In a future paper we plan to include a complete treatment of the geometric coefficients K_{ij} for the reactions between specific pairs of TDs. This modification will break the overall symmetry of the set of the twenty-four differential equations in such a way that equations for families 1 through 16 will be inequivalent to the equations for families 17 through 24. Therefore, the possibility of the global reduction behavior other than that predicted by (10) will be examined.

Acknowledgements This work was supported in part by the UC MICRO program in conjunction with Hughes Aircraft corporation, by the AFOSR through contract F49620-95-0394 (Dr. Gerald Witt contract monitor), by the NSF MRL program grant No. DMR-9123048, and by the Max Planck Society. Additional support for GEB was provided by an Alexander-von-Humboldt Fellowship.

Appendix A

In this appendix, we consider the addition of scattering reactions to the series of differential equations for TD kinetics. Equation (1), in principle, includes all possible reactions between TDs from family 1 with TDs of any other of the twenty-four families. Based on the analysis of Part I, we may only conclude that $K_{11} = K_{13} = 0$ because the TDs in these pairs have no relative motion with increasing film thickness. Some of the possible reactions in (1) correspond to scattering (fusion and annihilation have been treated in the main body of the text). For the case of scattering, it is important that

there is the conservation of Burgers vector during scattering reactions, this means that TDs of family 1 can appear only from scattered TDs from families 1 or 2.

Consider now an example of scattering. For the entry [(1, 2)-(5, 6)] in Table I.1, dislocations of family 1 are *produced* by scattering reactions. In differential form, the scattering may be represented as

$$\frac{\mathrm{d}\varrho_{1}}{\mathrm{d}h} = \beta_{1,5}^{1} K_{1,5} \varrho_{1} \varrho_{5} + \beta_{1,6}^{1} K_{1,6} \varrho_{1} \varrho_{6} + \beta_{2,5}^{1} K_{2,5} \varrho_{2} \varrho_{5} + \beta_{2,6}^{1} K_{2,6} \varrho_{2} \varrho_{6}, \tag{A1}$$

where, again, β_{ij}^k describes the probability that the reaction TDs from the *i*-th and *j*-th families form a TD from the *k*-th family. If only one TD is formed, then this is a fusion reaction, if two TDs result, then it is a scattering reaction. It was argued in Part I that for scattering reactions the following relation must be true:

$$\beta_{ij}^{k} + \beta_{ij}^{m} + \beta_{ij}^{i} + \beta_{ij}^{j} = 2, \tag{A2}$$

where, again families i and k have the same Burgers vector and families j and m have the same Burgers vector (but not the same \mathbf{b} as for families i and k). This relation simply reflects the conservation of the Burgers vectors of the reacting TDs, i.e., scattering reactions do not directly reduce ϱ_{T} . If there is no scattering, then $\beta_{ij}^k = \beta_{ij}^m = 0$ and $\beta_{ij}^i = \beta_{ij}^j = 1$. If there is scattering with overall equal probability, then $\beta_{ij}^k = \beta_{ij}^m = \beta_{ij}^i = \beta_{ij}^j = \beta_{ij}^j = \frac{\beta_{ij}^i}{2} = \frac{$

Now we can combine all contributions, in accordance with Table I.1, to the change of dislocation density of ϱ_1 .

$$\begin{split} \frac{\mathrm{d}\varrho_1}{\mathrm{d}h} &= (-1 + \beta_{1,2}^1) \, K_{1,2}\varrho_1\varrho_2 - K_{1,4}\varrho_1\varrho_4 \\ &\quad + (-1 + \beta_{1,5}^1) \, K_{1,5}\varrho_1\varrho_5 + \beta_{2,5}^1 K_{2,5}\varrho_2\varrho_5 \\ &\quad + (-1 + \beta_{1,6}^1) \, K_{1,6}\varrho_1\varrho_6 + \beta_{2,6}^1 K_{2,6}\varrho_2\varrho_6 \\ &\quad + (-1 + \beta_{1,7}^1) \, K_{1,7}\varrho_1\varrho_7 + \beta_{2,7}^1 K_{2,7}\varrho_2\varrho_7 \\ &\quad + (-1 + \beta_{1,8}^1) \, K_{1,8}\varrho_1\varrho_8 + \beta_{2,8}^1 K_{2,8}\varrho_2\varrho_8 \\ &\quad + (-1 + \beta_{1,9}^1) \, K_{1,9}\varrho_1\varrho_9 + \beta_{2,9}^1 K_{2,9}\varrho_2\varrho_9 \\ &\quad + (-1 + \beta_{1,10}^1) \, K_{1,10}\varrho_1\varrho_{10} + \beta_{2,10}^1 K_{2,10}\varrho_2\varrho_{10} - K_{1,11}\varrho_1\varrho_{11} - K_{1,12}\varrho_1\varrho_{12} \\ &\quad + (-1 + \beta_{1,13}^1) \, K_{1,13}\varrho_1\varrho_{13} + \beta_{2,13}^1 K_{2,13}\varrho_2\varrho_{13} \\ &\quad + (-1 + \beta_{1,14}^1) \, K_{1,14}\varrho_1\varrho_{14} + \beta_{2,14}^1 K_{2,14}\varrho_2\varrho_{14} - K_{1,15}\varrho_1\varrho_{15} - K_{1,16}\varrho_1\varrho_{16} \\ &\quad + (-1 + \beta_{1,17}^1) \, K_{1,17}\varrho_1\varrho_{17} + \beta_{2,17}^1 K_{2,17}\varrho_2\varrho_{17} \\ &\quad + (-1 + \beta_{1,18}^1) \, K_{1,18}\varrho_1\varrho_{18} + \beta_{2,18}^1 K_{2,18}\varrho_2\varrho_{18} - K_{1,19}\varrho_1\varrho_{19} - K_{1,20}\varrho_1\varrho_{20} \\ &\quad + (-1 + \beta_{1,21}^1) \, K_{1,21}\varrho_1\varrho_{21} + \beta_{2,21}^1 K_{2,21}\varrho_2\varrho_{21} \\ &\quad + (-1 + \beta_{1,22}^1) \, K_{1,22}\varrho_1\varrho_{22} + \beta_{2,22}^1 K_{2,22}\varrho_2\varrho_{22} - K_{1,23}\varrho_1\varrho_{23} - K_{1,24}\varrho_1\varrho_{24} \\ &\quad + K_{13,17}\varrho_{13}\varrho_{17} + K_{13,18}\varrho_{13}\varrho_{18} + K_{14,17}\varrho_{14}\varrho_{17} + K_{14,18}\varrho_{14}\varrho_{18} \, . \end{split}$$
 (A3)

The equations for densities of TDs from the other families will have a similar structure. Note that in the absence of scattering, (A3) transforms to (4).

Appendix B

This appendix provides the system of coupled first-order nonlinear ordinary differential equations for TD families in growing (001) epitaxial f.c.c. films.

$$\frac{1}{c} \frac{\mathrm{d}\tilde{\varrho}_{1}}{\mathrm{d}\tilde{h}} = -\tilde{\varrho}_{1}\tilde{\varrho}_{4} - \varkappa\tilde{\varrho}_{1}(\tilde{\varrho}_{11} + \tilde{\varrho}_{12} + \tilde{\varrho}_{15} + \tilde{\varrho}_{16} + \tilde{\varrho}_{19} + \tilde{\varrho}_{20} + \tilde{\varrho}_{23} + \tilde{\varrho}_{24})
+ \varkappa(\tilde{\varrho}_{13} + \tilde{\varrho}_{14})(\tilde{\varrho}_{17} + \tilde{\varrho}_{18}),$$
(B1)

$$\frac{1}{c} \frac{d\tilde{\varrho}_{2}}{d\tilde{h}} = -\tilde{\varrho}_{2}\tilde{\varrho}_{3} - \varkappa\tilde{\varrho}_{2}(\tilde{\varrho}_{11} + \tilde{\varrho}_{12} + \tilde{\varrho}_{15} + \tilde{\varrho}_{16} + \tilde{\varrho}_{19} + \tilde{\varrho}_{20} + \tilde{\varrho}_{23} + \tilde{\varrho}_{24})
+ \varkappa(\tilde{\varrho}_{9} + \tilde{\varrho}_{10}) (\tilde{\varrho}_{21} + \tilde{\varrho}_{22}),$$
(B2)

$$\frac{1}{c} \frac{d\tilde{\varrho}_{3}}{d\tilde{h}} = -\tilde{\varrho}_{2}\tilde{\varrho}_{3} - \varkappa\tilde{\varrho}_{3}(\tilde{\varrho}_{9} + \tilde{\varrho}_{10} + \tilde{\varrho}_{13} + \tilde{\varrho}_{14} + \tilde{\varrho}_{17} + \tilde{\varrho}_{18} + \tilde{\varrho}_{21} + \tilde{\varrho}_{22})
+ \varkappa(\tilde{\varrho}_{15} + \tilde{\varrho}_{16})(\tilde{\varrho}_{19} + \tilde{\varrho}_{20}),$$
(B3)

$$\frac{1}{c} \frac{\mathrm{d}\tilde{\varrho}_4}{\mathrm{d}\tilde{h}} = -\tilde{\varrho}_1\tilde{\varrho}_4 - \varkappa\tilde{\varrho}_4(\tilde{\varrho}_9 + \tilde{\varrho}_{10} + \tilde{\varrho}_{13} + \tilde{\varrho}_{14} + \tilde{\varrho}_{17} + \tilde{\varrho}_{18} + \tilde{\varrho}_{21} + \tilde{\varrho}_{22})
+ \varkappa(\tilde{\varrho}_{11} + \tilde{\varrho}_{12}) \left(\tilde{\varrho}_{23} + \tilde{\varrho}_{24}\right),$$
(B4)

$$\frac{1}{c} \frac{\mathrm{d}\tilde{\varrho}_{5}}{\mathrm{d}\tilde{h}} = -\tilde{\varrho}_{5}\tilde{\varrho}_{8} - \varkappa\tilde{\varrho}_{5}(\tilde{\varrho}_{11} + \tilde{\varrho}_{12} + \tilde{\varrho}_{15} + \tilde{\varrho}_{16} + \tilde{\varrho}_{17} + \tilde{\varrho}_{18} + \tilde{\varrho}_{21} + \tilde{\varrho}_{22})
+ \varkappa(\tilde{\varrho}_{9} + \tilde{\varrho}_{10}) (\tilde{\varrho}_{19} + \tilde{\varrho}_{20}),$$
(B5)

$$\frac{1}{c} \frac{d\tilde{\varrho}_{6}}{d\tilde{h}} = -\tilde{\varrho}_{6}\tilde{\varrho}_{7} - \varkappa\tilde{\varrho}_{6}(\tilde{\varrho}_{11} + \tilde{\varrho}_{12} + \tilde{\varrho}_{15} + \tilde{\varrho}_{16} + \tilde{\varrho}_{17} + \tilde{\varrho}_{18} + \tilde{\varrho}_{21} + \tilde{\varrho}_{22})
+ \varkappa(\tilde{\varrho}_{13} + \tilde{\varrho}_{14}) (\tilde{\varrho}_{23} + \tilde{\varrho}_{24}),$$
(B6)

$$\frac{1}{c} \frac{\mathrm{d}\tilde{\varrho}_{7}}{\mathrm{d}\tilde{h}} = -\tilde{\varrho}_{6}\tilde{\varrho}_{7} - \varkappa\tilde{\varrho}_{7}(\tilde{\varrho}_{9} + \tilde{\varrho}_{10} + \tilde{\varrho}_{13} + \tilde{\varrho}_{14} + \tilde{\varrho}_{19} + \tilde{\varrho}_{20} + \tilde{\varrho}_{23} + \tilde{\varrho}_{24})
+ \varkappa(\tilde{\varrho}_{11} + \tilde{\varrho}_{12}) (\tilde{\varrho}_{17} + \tilde{\varrho}_{18}),$$
(B7)

$$\frac{1}{c} \frac{\mathrm{d}\tilde{\varrho}_{8}}{\mathrm{d}\tilde{h}} = -\tilde{\varrho}_{5}\tilde{\varrho}_{8} - \varkappa\tilde{\varrho}_{8}(\tilde{\varrho}_{9} + \tilde{\varrho}_{10} + \tilde{\varrho}_{13} + \tilde{\varrho}_{14} + \tilde{\varrho}_{19} + \tilde{\varrho}_{20} + \tilde{\varrho}_{23} + \tilde{\varrho}_{24})
+ \varkappa(\tilde{\varrho}_{15} + \tilde{\varrho}_{16})(\tilde{\varrho}_{21} + \tilde{\varrho}_{22}),$$
(B8)

$$\frac{1}{c} \frac{\mathrm{d}\tilde{\varrho}_{9}}{\mathrm{d}\tilde{h}} = -\tilde{\varrho}_{9}\tilde{\varrho}_{12} - \varkappa\tilde{\varrho}_{9}(\tilde{\varrho}_{3} + \tilde{\varrho}_{4} + \tilde{\varrho}_{7} + \tilde{\varrho}_{8} + \tilde{\varrho}_{19} + \tilde{\varrho}_{20} + \tilde{\varrho}_{21} + \tilde{\varrho}_{22})
+ \varkappa(\tilde{\varrho}_{1} + \tilde{\varrho}_{2}) (\tilde{\varrho}_{23} + \tilde{\varrho}_{24}),$$
(B9)

$$\frac{1}{c} \frac{d\tilde{\varrho}_{10}}{d\tilde{h}} = -\tilde{\varrho}_{10}\tilde{\varrho}_{11} - \varkappa \tilde{\varrho}_{10}(\tilde{\varrho}_3 + \tilde{\varrho}_4 + \tilde{\varrho}_7 + \tilde{\varrho}_8 + \tilde{\varrho}_{19} + \tilde{\varrho}_{20} + \tilde{\varrho}_{21} + \tilde{\varrho}_{22})
+ \varkappa (\tilde{\varrho}_5 + \tilde{\varrho}_6) (\tilde{\varrho}_{17} + \tilde{\varrho}_{18}),$$
(B10)

$$\frac{1}{c} \frac{d\tilde{\varrho}_{11}}{d\tilde{h}} = -\tilde{\varrho}_{10}\tilde{\varrho}_{11} - \varkappa \tilde{\varrho}_{11}(\tilde{\varrho}_1 + \tilde{\varrho}_2 + \tilde{\varrho}_5 + \tilde{\varrho}_6 + \tilde{\varrho}_{17} + \tilde{\varrho}_{18} + \tilde{\varrho}_{23} + \tilde{\varrho}_{24})
+ \varkappa (\tilde{\varrho}_3 + \tilde{\varrho}_4) (\tilde{\varrho}_{21} + \tilde{\varrho}_{22}),$$
(B11)

$$\frac{1}{c} \frac{\mathrm{d}\tilde{\varrho}_{12}}{\mathrm{d}\tilde{h}} = -\tilde{\varrho}_{9}\tilde{\varrho}_{12} - \varkappa \tilde{\varrho}_{12}(\tilde{\varrho}_{1} + \tilde{\varrho}_{2} + \tilde{\varrho}_{5} + \tilde{\varrho}_{6} + \tilde{\varrho}_{17} + \tilde{\varrho}_{18} + \tilde{\varrho}_{23} + \tilde{\varrho}_{24})
+ \varkappa (\tilde{\varrho}_{7} + \tilde{\varrho}_{8}) (\tilde{\varrho}_{19} + \tilde{\varrho}_{20}),$$
(B12)

$$\frac{1}{c} \frac{\mathrm{d}\tilde{\varrho}_{13}}{\mathrm{d}\tilde{h}} = -\tilde{\varrho}_{13}\tilde{\varrho}_{16} - \varkappa \tilde{\varrho}_{13}(\tilde{\varrho}_3 + \tilde{\varrho}_4 + \tilde{\varrho}_7 + \tilde{\varrho}_8 + \tilde{\varrho}_{17} + \tilde{\varrho}_{18} + \tilde{\varrho}_{23} + \tilde{\varrho}_{24})
+ \varkappa (\tilde{\varrho}_5 + \tilde{\varrho}_6) (\tilde{\varrho}_{21} + \tilde{\varrho}_{22}),$$
(B13)

$$\frac{1}{c} \frac{\mathrm{d}\tilde{\varrho}_{14}}{\mathrm{d}\tilde{h}} = -\tilde{\varrho}_{14}\tilde{\varrho}_{15} - \varkappa \tilde{\varrho}_{14}(\tilde{\varrho}_3 + \tilde{\varrho}_4 + \tilde{\varrho}_7 + \tilde{\varrho}_8 + \tilde{\varrho}_{17} + \tilde{\varrho}_{18} + \tilde{\varrho}_{23} + \tilde{\varrho}_{24})
+ \varkappa (\tilde{\varrho}_1 + \tilde{\varrho}_2) (\tilde{\varrho}_{19} + \tilde{\varrho}_{29}),$$
(B14)

$$\frac{1}{c} \frac{\mathrm{d}\tilde{\varrho}_{15}}{\mathrm{d}\tilde{h}} = -\tilde{\varrho}_{14}\tilde{\varrho}_{15} - \varkappa \tilde{\varrho}_{15}(\tilde{\varrho}_1 + \tilde{\varrho}_2 + \tilde{\varrho}_5 + \tilde{\varrho}_6 + \tilde{\varrho}_{19} + \tilde{\varrho}_{20} + \tilde{\varrho}_{21} + \tilde{\varrho}_{22})
+ \varkappa (\tilde{\varrho}_7 + \tilde{\varrho}_8) (\tilde{\varrho}_{23} + \tilde{\varrho}_{24}),$$
(B15)

$$\frac{1}{c} \frac{\mathrm{d}\tilde{\varrho}_{16}}{\mathrm{d}\tilde{h}} = -\tilde{\varrho}_{13}\tilde{\varrho}_{16} - \varkappa \tilde{\varrho}_{16}(\tilde{\varrho}_1 + \tilde{\varrho}_2 + \tilde{\varrho}_5 + \tilde{\varrho}_6 + \tilde{\varrho}_{19} + \tilde{\varrho}_{20} + \tilde{\varrho}_{21} + \tilde{\varrho}_{22})
+ \varkappa (\tilde{\varrho}_3 + \tilde{\varrho}_4) (\tilde{\varrho}_{17} + \tilde{\varrho}_{18}),$$
(B16)

$$\frac{1}{c} \frac{\mathrm{d}\tilde{\varrho}_{17}}{\mathrm{d}\tilde{h}} = -\tilde{\varrho}_{17}\tilde{\varrho}_{20} - \varkappa\tilde{\varrho}_{17}(\tilde{\varrho}_3 + \tilde{\varrho}_4 + \tilde{\varrho}_5 + \tilde{\varrho}_6 + \tilde{\varrho}_{11} + \tilde{\varrho}_{12} + \tilde{\varrho}_{13} + \tilde{\varrho}_{14})
+ \varkappa(\tilde{\varrho}_1 + \tilde{\varrho}_2) (\tilde{\varrho}_{15} + \tilde{\varrho}_{16}),$$
(B17)

$$\frac{1}{c} \frac{\mathrm{d}\tilde{\varrho}_{18}}{\mathrm{d}\tilde{h}} = -\tilde{\varrho}_{18}\tilde{\varrho}_{19} - \varkappa\tilde{\varrho}_{18}(\tilde{\varrho}_3 + \tilde{\varrho}_4 + \tilde{\varrho}_5 + \tilde{\varrho}_6 + \tilde{\varrho}_{11} + \tilde{\varrho}_{12} + \tilde{\varrho}_{13} + \tilde{\varrho}_{14})
+ \varkappa(\tilde{\varrho}_7 + \tilde{\varrho}_8)(\tilde{\varrho}_9 + \tilde{\varrho}_{10}),$$
(B18)

$$\frac{1}{c} \frac{\mathrm{d}\tilde{\varrho}_{19}}{\mathrm{d}\tilde{h}} = -\tilde{\varrho}_{18}\tilde{\varrho}_{19} - \varkappa \tilde{\varrho}_{19}(\tilde{\varrho}_1 + \tilde{\varrho}_2 + \tilde{\varrho}_7 + \tilde{\varrho}_8 + \tilde{\varrho}_9 + \tilde{\varrho}_{10} + \tilde{\varrho}_{15} + \tilde{\varrho}_{16})
+ \varkappa (\tilde{\varrho}_3 + \tilde{\varrho}_4) (\tilde{\varrho}_{13} + \tilde{\varrho}_{14}),$$
(B19)

$$\frac{1}{c} \frac{\mathrm{d}\tilde{\varrho}_{20}}{\mathrm{d}\tilde{h}} = -\tilde{\varrho}_{17}\tilde{\varrho}_{20} - \varkappa \tilde{\varrho}_{20}(\tilde{\varrho}_1 + \tilde{\varrho}_2 + \tilde{\varrho}_7 + \tilde{\varrho}_8 + \tilde{\varrho}_9 + \tilde{\varrho}_{10} + \tilde{\varrho}_{15} + \tilde{\varrho}_{16})
+ \varkappa (\tilde{\varrho}_5 + \tilde{\varrho}_6) (\tilde{\varrho}_{11} + \tilde{\varrho}_{12}),$$
(B20)

$$\frac{1}{c} \frac{\mathrm{d}\tilde{\varrho}_{21}}{\mathrm{d}\tilde{h}} = -\tilde{\varrho}_{21}\tilde{\varrho}_{24} - \varkappa\tilde{\varrho}_{21}(\tilde{\varrho}_3 + \tilde{\varrho}_4 + \tilde{\varrho}_5 + \tilde{\varrho}_6 + \tilde{\varrho}_9 + \tilde{\varrho}_{10} + \tilde{\varrho}_{15} + \tilde{\varrho}_{16})
+ \varkappa(\tilde{\varrho}_1 + \tilde{\varrho}_2)(\tilde{\varrho}_{11} + \tilde{\varrho}_{12}),$$
(B21)

$$\frac{1}{c} \frac{\mathrm{d}\tilde{\varrho}_{22}}{\mathrm{d}\tilde{h}} = -\tilde{\varrho}_{22}\tilde{\varrho}_{23} - \varkappa\tilde{\varrho}_{22}(\tilde{\varrho}_3 + \tilde{\varrho}_4 + \tilde{\varrho}_5 + \tilde{\varrho}_6 + \tilde{\varrho}_9 + \tilde{\varrho}_{10} + \tilde{\varrho}_{15} + \tilde{\varrho}_{16})
+ \varkappa(\tilde{\varrho}_7 + \tilde{\varrho}_8) (\tilde{\varrho}_{13} + \tilde{\varrho}_{14}),$$
(B22)

$$\frac{1}{c} \frac{\mathrm{d}\tilde{\varrho}_{23}}{\mathrm{d}\tilde{h}} = -\tilde{\varrho}_{22}\tilde{\varrho}_{23} - \varkappa\tilde{\varrho}_{23}(\tilde{\varrho}_1 + \tilde{\varrho}_2 + \tilde{\varrho}_7 + \tilde{\varrho}_8 + \tilde{\varrho}_{11} + \tilde{\varrho}_{12} + \tilde{\varrho}_{13} + \tilde{\varrho}_{14})
+ \varkappa(\tilde{\varrho}_3 + \tilde{\varrho}_4)(\tilde{\varrho}_9 + \tilde{\varrho}_{10}),$$
(B23)

$$\frac{1}{c} \frac{d\tilde{\varrho}_{24}}{d\tilde{h}} = -\tilde{\varrho}_{21}\tilde{\varrho}_{24} - \varkappa \tilde{\varrho}_{24}(\tilde{\varrho}_1 + \tilde{\varrho}_2 + \tilde{\varrho}_7 + \tilde{\varrho}_8 + \tilde{\varrho}_{11} + \tilde{\varrho}_{12} + \tilde{\varrho}_{13} + \tilde{\varrho}_{14})
+ \varkappa (\tilde{\varrho}_5 + \tilde{\varrho}_6) (\tilde{\varrho}_{15} + \tilde{\varrho}_{16}).$$
(B24)

The equations in this system were derived in the same way as (8). Normalized TD densities $\tilde{\varrho}_i = \varrho_i r_{\rm A}^2$ and thickness $\tilde{h} = h/r_{\rm A}$ are used in this system of equations. The coefficient $\varkappa = r_{\rm F}/r_{\rm A}$ denotes the relative radius for fusion reactions. The parameter c describes the dependence of TD motion on their inclination with respect to the surface normal. For perpendicular orientations, c = 0, for large inclination, c tends to infinity. For the real case of (001) epitaxy, $c \approx 2$.

References

- [1] A. E. Romanov, W. Pompe, G. Beltz, and J. S. Speck, phys. stat. sol. (b) 198, 599 (1996).
- [2] P. SHELDON, K. M. JONES, M. M. AL-JASSIM, and B. G. YACOBI, J. appl. Phys. 63, 5609 (1988).
- [3] M. TACHIKAWA and M. YAMAGUCHI, Appl. Phys. Letters 56, 484 (1990).
- [4] R. Beanland, D. J. Dunstan, and P. J. Goodhew, Adv. Phys. 45, 87 (1996).
- [5] J. S. SPECK, M. A. BREWER, G. E. BELTZ, A. E. ROMANOV, and W. POMPE, J. appl. Phys. 80, 3808 (1996).